Tittle: Chromosome 10q24.32 Variants Associate with Brain Arterial Diameters in Diverse Populations: A Genome-Wide Association Study

Authors: Minghua Liu[1], Farid Khasiyev[2], Sanjeev Sariya[1,3,4], Antonio Spagnolo-Allende[1], Danurys L Sanchez[1,3,4], Howard Andrews[5], Qiong Yang[6], Alexa Beiser[6], Ye Qiao[7], Emy A Thomas[8], Jose Rafael Romero[9], Tatjana Rundek[10,11,12], Adam Brickman[1,3,4] , Jennifer J Manly[1,3,4] , Mitchell SV Elkind[1,13], Sudha Seshadri[9,14], Christopher Chen[15], Ralph L Sacco[10,11,12], Saima Hilal[15], Bruce A Wasserman[7,16], Giuseppe Tosto[1,3,4], Myriam Fornage[8,17], Jose Gutierrez[1].

Affiliations:
1 Department of Neurology, Vagelos College of Physicians and Surgeons, Columbia University, New York, NY, USA
2 Department of Neurology, Saint Louis University School of Medicine, St. Louis, MO, USA
3 Taub Institute for Research on Alzheimer's Disease and the Aging Brain, Vagelos College of Physicians and Surgeons, Columbia University, New York, NY, USA
4 The Gertrude H. Sergievsky Center, Vagelos College of Physicians and Surgeons, Columbia University, New York, NY, USA
5 Biostatistics Department, Mailman School of Public Health, Columbia University, New York, NY, USA
6 Department of Biostatistics, School of Public Health, Boston University, Boston, MA, USA
7 Johns Hopkins University School of Medicine, Baltimore, MD, USA
8 Brown Foundation Institute of Molecular Medicine, Mc Govern Medical School, The University of Texas Health Science Center at Houston, Houston, TX, USA
9 Department of Neurology, Boston University School of Medicine, Boston, MA, USA
10 Department of Neurology, University of Miami Miller School of Medicine, Miami, FL, USA
11 Department of Public Health Sciences, University of Miami Miller School of Medicine, Miami, FL, USA
12 Evelyn F. McKnight Brain Institute, University of Miami Miller School of Medicine, Miami, FL, USA
13 Department of Epidemiology, Mailman School of Public Health, Columbia University, New York, NY, USA
14 The Glenn Biggs Institute for Alzheimer's and Neurodegenerative Diseases, University of Texas Health Sciences Center, San Antonio, TX, USA
15 Memory Aging and Cognition Center, Department of Pharmacology, Yong Loo Lin School of Medicine, National University of Singapore, Singapore
16 University of Maryland School of Medicine, Baltimore, MD, USA
17 Human Genetics Center, School of Public Health, The University of Texas Health Science Center at Houston, Houston, TX, USA

Contact author:
Jose Gutierrez, MD, MPH.
Address: 710 W 168th Street, 6th floor, Suite 639
New York, NY, 10032.
Email: jg3233@cumc.columbia.edu
Phone: (212) 305-1710; Fax: (212) 305-165

Author Name	Email Address
Minghua Liu	ml3883@cumc.columbia.edu
Farid Khasiyev	farid.khasiyev@health.slu.edu
Sanjeev Sariya	ss5505@cumc.columbia.edu
Antonio Spagnolo-Allende	ajs2363@cumc.columbia.edu
Danurys L Sanchez	dls167@cumc.columbia.edu
Howard Andrews	Howard.Andrews@nyspi.columbia.edu
Qiong Yang	qyang@bu.edu
Alexa Beiser	alexab@bu.edu
Ye Qiao	yqiao4@jhmi.edu
Emy A Thomas	Emy.Anu.Thomas@uth.tmc.edu
Jose Rafael Romero	joromero@bu.edu
Tatjana Rundek	TRundek@med.miami.edu
Adam Brickman	amb2139@cumc.columbia.edu
Jennifer J Manly	jjm71@cumc.columbia.edu
Mitchell SV Elkind	mse13@cumc.columbia.edu
Sudha Seshadri	seshadri@uthscsa.edu
Christopher Chen	phccclh@nus.edu.sg
Ralph L Sacco	rsacco@med.miami.edu
Saima Hilal	saimahilal@nus.edu.sg
Bruce A Wasserman	BWasser@som.umaryland.edu
Giuseppe Tosto	gt2260@cumc.columbia.edu
Myriam Fornage	Myriam.Fornage@uth.tmc.edu
Jose Gutierrez	jg3233@cumc.columbia.edu

Abstract

Background: Brain arterial diameters are novel imaging biomarkers of cerebrovascular disease, cognitive decline and dementia. Traditional vascular risk factors have been associated with brain arterial diameters but whether there may be genetic determinants of brain arterial diameters is unknown.

Results: We studied 4150 participants from six geographically diverse population-based cohorts (40% European, 14% African, 22% Hispanic, 24% Asian ancestries). We measured brain arterial diameters for 13 segments and averaged them to obtain a global measure of brain arterial diameters as well as the posterior and anterior circulations. A genome-wide association study (GWAS) revealed 14 variants at one locus associated with global brain arterial diameter at genome-wide significance ($P<5\times10^{-8}$) (top SNP, rs7921574; β =0.06, $P=1.54\times10^{-8}$). This locus mapped to an intron of *CNNM2*. A trans-ancestry GWAS meta-analysis identified two more loci at *NT5C2* (rs10748839; $P=2.54\times10^{-8}$) and at *AS3MT* (rs10786721; $P=4.97\times10^{-8}$), associated with global brain arterial diameter. In addition, two SNPs co-localized with expression of *CNNM2* (rs7897654, β=0.12, $P=6.17\times10^{-7}$) and *AL356608.1* (rs10786719, β =-0.17, $P=6.60\times10^{-6}$) in brain tissue. For the posterior brain arterial diameter, two variants at one locus mapped to an intron of *TCF25* were identified (top SNP, rs35994878; β =0.11, $P=2.94\times10^{-8}$). For the anterior brain arterial diameter, one locus at *ADAP1* was identified in trans-ancestry genome-wide association analysis (rs34217249; $P=3.11\times10^{-8}$).

Conclusion: Our study reveals three novel risk loci (CNNM2, NT5C2 and AS3MT) associated with brain arterial diameters. Our finding may elucidate the mechanisms by which brain arterial diameters influence the risk of stroke and dementia.

Key words: Larger brain arterial diameters, Genome-wide association studies, Chromosome 10q24.32, Cyclin and CBS Domain Divalent Metal Cation Transport Mediator 2 (CNNM2)

Background

Dolichoectasia has been defined by elongated and tortuous arteries [1] and it is usually associated with smoking, male sex and aging.[2] The diagnosis of dolichoectasia has been historically ascertained by visual inspection of neuroimaging or more recently using a fixed arterial diameter cutoffs for the basilar artery.[3] Although these methods are easy to use, they simplify the biological meaning of the continuum of intracranial arterial diameters in brain health and neglect arterial-size expectations based on age, sex and head size.[4] Therefore, we proposed and validated the principle that arterial diameters measured continuously and adjusted for head size relate to health outcomes in a non-linear fashion and that people with very small or very large arterial diameters are at a higher risk of vascular events.[5] Furthermore, dilated brain arterial diameters are associated with a higher risk of dementia [6] and steeper cognitive decline.[7] Smaller arterial diameters causing stenosis, usually related to atherosclerosis, are intuitively related to adverse health outcomes [8,9] but less is known about the underlying nature of dilated brain arteries.

Larger arterial diameters have been described in people with connective tissue disorders such as Marfan syndrome,[10] Ehlers-Danlos,[11] and Arterial Tortuosity Syndrome,[12] among others. These monogenic diseases are usually rare and detected in younger patients. Furthermore, there is clear association between larger arterial diameters and vascular risk factors, especially hypertension.[13,14] Although hypertension is highly prevalent in elderly populations, the heterogeneity of brain arterial phenotypes in people with vascular risk factors suggests that a specific genetic profile might partially be responsible for higher risk of brain arterial dilatation. Consequently, we hypothesize that in the general population less pathogenic but more frequent genetic variants may relate to brain arterial diameters. Identifying such a genetic profile may shed light into possible mechanistic links between large brain arterial diameters and the observed brain outcomes. To test our hypothesis, we leveraged diverse population cohorts within and outside the United States to investigate associations between brain arterial diameters and Alzheimer's disease, stroke, and white matter hyperintensities volume.

Results

Multi-ancestry GWAS Identifies a Novel Locus Associated with Brain Arterial Diameter

We conducted a multi-ancestry GWAS for brain arterial diameter levels in 4150 participants, including 1650 from European, 583 from African, 920 from Hispanic, and 997 from Asian ancestries. Mean age of the participants across studies ranged from 70 to 76 years, with proportions of women ranging from 52 to 64%. Detailed demographic information is presented in Table 1.

We identified 14 variants at one locus associated with global brain arterial diameter at genome-wide significance ($P<5\times10^{-8}$; Figure 1A). This locus mapped to an intron of *CNNM2* (Cyclin and CBS Domain Divalent Metal Cation Transport Mediator 2). One copy of the C allele (minor allele frequency [MAF], 0.42) for the lead single-nucleotide polymorphism (SNP) rs7921574 was associated with 6% increased global brain arterial diameter ($P=1.54\times10^{-8}$) (Table 2; Figure S1A). We also identified 2 intronic variants in *TCF25* (Transcription Factor 25) associated with posterior brain arterial diameter at genome-wide significance (Figure 1B). One copy of the C allele (MAF= 0.29) for the lead SNP rs35994878 was associated with 11% increased posterior brain arterial diameter ($P=2.94\times10^{-8}$) (Table 2; Figure S1B). We did not observe any genome-wide significant association for anterior brain arterial diameter (Figure 1C). No genomic

inflation was observed for any of the brain arterial diameter analyses (Figure S2). We also performed ancestry-specific regional Manhattan plots for top SNPs in global (rs7921574), anterior (rs7921574), and posterior (rs35994878) diameter meta-analysis, respectively (Figure S3, S4, and S5), but did not observe ancestry-specific genome-wide significant associations.

In the trans-ancestry genome-wide association analysis for global brain arterial diameter, in addition to SNPs in *CNNM2*, we identified one genome-wide significant SNP near *NT5C2* (rs10748839; $P=2.54\times10^{-8}$) and one in *AS3MT* (rs10786721; $P=4.97\times10^{-8}$). All were located within 10q24.32. For anterior brain arterial diameter, we identified one locus at *ADAP1* (rs34217249; $P=3.11\times10^{-8}$) (Table 3). In the Hispanic-specific analysis, we identified a genome-wide significant locus at *LOC107986223* for global brain arterial diameter; three loci at *TGFBR2, LOC105374506,* and *LOC105376292* for posterior brain arterial diameter (Table S5). We did not observe genome-wide significant association in European, African, or Asian ancestries (Table S3, S4 and S6) for global, anterior, or posterior brain arterial diameter. No genomic inflation was observed in trans-ancestry analysis (Figure S6, S7, and S8).

Variant Effects Predictions on Protein Coding Sequence

We investigated the predicted deleterious effects of brain arterial diameter-associated loci using the Combined Annotation Dependent Depletion (CADD) scores. The SNPs and their proxies with CADD scores are shown in Table 2 and Table 3. We did not observe significant CADD score among the genome-wide significant loci associated with brain arterial diameter. A SNP associated with posterior brain arterial diameter in the *RAD52* region (rs140934041) showed significant CADD score (13.45) in Hispanic-specific analysis (Table S5). Additionally, SNPs associated with anterior brain arterial diameter in the *RAPGEF4* and posterior brain arterial diameter in *PODXL* region showed significant CADD scores (rs2290378, 16.31; rs888608, 16.63) in Asian-specific analysis (Table S6).

Gene-Based Association Test and Gene-Set Enrichment

The Multi-Marker Analysis of GenoMic Annotation gene-based association analysis identified one locus associated with global brain arterial diameter ($P<1.50\times10^{-5}$) (Table S7). The significant associations for global brain arterial diameter included the GWAS located at *AS3MT, CNNM2, NT5C2, ARL3, TMEM180, C10orf32* and *C10orf32-ASMT*. Genes mapped to GWAS associations with $P<1\times10^{-5}$ were further investigated for gene-set enrichment (Table S8). Three genome-wide significant loci for global brain arterial diameter, *AS3MT, CNNM2* and *NT5C2*, were enriched in the white matter lesion progression gene set from GWAS catalog database (adjusted $P=7.60\times10^{-7}$).

Tissue-Specific Colocalization Analyses

We performed colocalization analysis for the locus identified in the GWAS and MTAG analysis with gene expression using Genotype-Tissue Expression v8 eQTL data (Table S9). We identified SNPs associated with *AS3MT* and *C10orf32* expression and global brain arterial diameter in all 13 brain tissues. We also identified SNPs at TMEM180 in caudate basal ganglia, cerebellar hemisphere, nucleus accumbent basal ganglia, putamen basal ganglia, and spinal cord cervical c-1; SNPs at *CNNM2* in caudate basal ganglia tissues and SNPs at *NT5C2* and *ARL3* in cerebellum tissue, which colocalized with global brain arterial diameter. We also performed a transcriptome-wide association analysis for the loci identified in the GWAS with gene expression using

BrainMeta project data in global, anterior, and posterior brain arterial diameter (Table 4). At the transcriptome-wide significance level ($P<8.4\times10^{-6}$), we identified SNPs associated with CNNM2 ($P=6.17\times10^{-7}$) and *AL356608.1* ($P=6.6\times10^{-6}$) expression in global brain arterial diameter (Figure 2A). We did not observe transcriptome-wide significant association in anterior or posterior brain arterial diameter (Figure 2B, 2C).

Causal Pathway from Brain Arterial Diameter to Alzheimer's disease, stroke, and white matter hyperintensities volume

To establish a causal pathway from brain arterial diameter to Alzheimer's disease, stroke, and white matter hyperintensities volume, we performed a Mendelian Randomization (MR) analysis (Table S10, S11). We did not observe any association of brain arterial diameter with Alzheimer's disease, stroke, or white matter hyperintensities volume.

Pleiotropic Locus for Anterior and Posterior Brain Arterial Diameter

MTAG analysis used the fixed-effect meta-analysis estimates for anterior and posterior brain arterial diameter. Since global brain arterial diameter is the average of anterior and posterior brain arterial diameter, the global estimate was excluded from multivariate analysis. No genomic inflation was observed in trans-ancestry analysis (Figure S9). MTAG results of joint analysis brain arterial diameter did not show any genome-wide significant SNPs (Table S12, S13).

Discussion

This is the first study to examine the genetic determinants of brain arterial diameter in an ancestrally diverse population, where we identified associations of novel genetic loci with brain arterial diameter genetic architecture. Beyond mapping to the nearest genes, we also showed the biological impact of our findings using in silico functional analyses. Our results demonstrated that multiple genetic loci were coupled with gene expression information, which imply biologically relevant pathways.

We identified a novel brain arterial diameter locus at 10q24.32 mapped to *CNNM2*. *CNNM2* encodes Cyclin M2, which is a member of magnesium (Mg^{2+}) transporters. As an abundant intracellular divalent cation in the human body, magnesium (Mg^{2+}) plays an important role in numerous biological processes such as the synthesis of RNA, DNA and protein, and the production and storage of cellular energy [42]. *CNNM2* is involved in brain development, neurological functioning and Mg^{2+} homeostasis [43]. Heterozygous variants in the *CNNM2* gene can cause renal hypomagnesemia (HOMG6 [MIM 613882]), seizures, and intellectual disability (HOMGSMR1 [MIM 616418]) [44]. In our study, variant rs7897654 was associated with decreased brain arterial diameter ($\beta=-0.06$) and an increased *CNNM2* expression ($\beta=0.02$) (Table 4). The variant rs7897654 colocalized with eQTLS of *CNNM2*, confirming its functional relationship to this gene. Our study also identified a variant in *TCF25* associated at genome-wide significance with posterior brain arterial diameter. *TCF25* is a member of the basic helix-loop-helix (bHLH) family of transcription factors that are important in embryonic development [45]. These two results suggest that the effects of these genetic variants on arterial size might be present early in life, but how aging interacts with these variants remains unknown.

The *NT5C2* encodes a phosphatase involved in cellular purine metabolism, which is associated with disorders characterized by psychiatric and psychomotor disturbances [46,47]. *NT5C2* has a

high affinity for adenosine monophosphate and is involved in the extensive transcriptional programming which regulates cell maintenance, proliferation, migration, and differentiation during neurodevelopment [48-51]. *NT5C2* has also been shown to negatively regulate phosphorylation of the alpha subunit of 5'-adenosine monophosphate-activated protein kinase (AMPK alpha) and protein translation[52]. Studies in the Chinese Han population report that *NT5C2* rs2148198 is associated with coronary heart disease susceptibility, and *NT5C2* rs11191580 is associated with schizophrenia and symptom severity [53,54]. In addition, a zebrafish study provides evidence that *NT5C2* and *CNNM2* are most likely the causal genes within a blood pressure locus at the 10q24.32 [55]. Our trans-ancestry GWAS analysis identified a significant variant rs10748839, mapped on the 2KB upstream of *NT5C2*, which is promoter variant that control expression of *NT5C2* [68].

The *AS3MT* gene, located in 10q24.32, encodes a cytosolic protein which is a cysteine rich enzyme that transfers a methyl group from S-adenosyl-L-methionine to trivalent arsenical [56,57]. *AS3MT* plays an important role in catalysis of biomethylation of arsenic in vivo and in vitro. *AS3MT* is mainly expressed in human adrenal glands, liver, heart, kidney, and brain [58]. Additionally, *AS3MT* expression is highly expressed in adult human neurons and astrocytes during human stem cell differentiation toward neuronal fates and in brains of patients with schizophrenia compared with controls [59] and with attention deficit or hyperactivity disorder[60]. Notably, *AS3MT* rs7085104 as a schizophrenia-associated risk SNP altered striatal dopamine synthesis capacity Moreover, the *AS3MT-CNNM2-NT5C2* gene cluster region is involved in etiology and pathogenesis of schizophrenia and the three genes have been confirmed as schizophrenia susceptibility gene cluster [61,62]. Our study identified *AS3MT* rs10786721 variants with genome-wide significance in global brain arterial diameter. In addition, *AS3MT* rs72841270 is a lead variant associated with global brain arterial diameter in Hispanic-specific population. Whether neuronal connectivity or network formation indirectly or directly impacts brain arterial diameters is unclear but should be further studied.

Lysosomes play a critical role in maintenance of the integrity of neuronal function, and mutations in genes that contribute to lysosome formation, transport, and activity are associated with neurodegenerative disorders [63,64]. Recently, the multi-subunit complex, BLOC-one-related complex (BORC), has been shown to be involved in positioning lysosomes within the cytoplasm, although the consequences of altered BORC function in adult animals have not been established [65,66]. A study in mice identifies *BORCS7* (*C10orf32*) as a central factor in axonal transport of lysosomes and a possible target for improving disease-related disturbances in this important function; additionally, the Q87X mutation in the *BORCS7* subunit results in motor deficits and dystrophic axonopathy in mice [67]. In our gene-based MAGMA analysis, the significant associations for global brain arterial diameter included *AS3MT*, *C10orf32*, *CNNM2* and *NT5C2*; we suspect that this four-gene cluster region may be involved with the etiology and pathogenesis of brain arterial diameter, but the underlying mechanism is not clear.

Our study is the first to explore the risk variants of brain arterial diameter in a large multi-ancestry GWAS. We detected novel SNPs located in genomic region 10q24.32 which are associated with brain arterial diameter. Due to the modest sample sizes of African, Asian, and Hispanic participants, the statistical power to detect ancestry-specific associations or functional associations in these ancestries were limited. Similarly, disentangling the effects of these variants

on overall brain health versus AD specific pathways is difficult without functional analyses of genes related to arterial diameters, but exploring such pathways may reveal novel vascular contribution to Alzheimer's disease and related dementias. Based on our results, we anticipate that the association between these genetic variants and brain arterial diameters will be consistent across populations, although the effect size might vary given the presence of common confounders such as vascular risk factors and environmental exposures.

Conclusions

In summary, we identified a novel genome-wide significant locus for brain arterial diameter, *CNNM2*, *NT5C2* and *AS3MT*, in a large multi-ancestry population. Our study provides a potential biological mechanism for the association between 10q24.32 variation and brain arterial diameter. Identifying genes associated with these loci and their function may help us to elucidate the mechanism by which brain arterial diameters may influence cerebrovascular health.

Methods

Sampled populations

Atherosclerosis Risk in Communities (ARIC) study

The ARIC study is a population-based prospective cohort study of vascular risks and includes 15,792 persons aged 45-64 years at baseline (1987-89), randomly chosen from four US communities.[15] Cohort members completed seven clinic examinations, conducted between 1987 and 2019. Written informed consent was provided by all study participants, and the study design and methods were approved by institutional review boards at the collaborating medical institutions (The Johns Hopkins University, Wake Forest University, University of Mississippi Medical Center, and University of Minnesota). Dementia and dementia subtypes were adjudicated beginning in 2011 using in-person interviews and cognitive testing, chart reviews and telephone surveys.[16]

The Northern Manhattan Study (NOMAS)

The NOMAS is an ongoing prospective cohort initially focused on determining the incidence of stroke and vascular events in a diverse urban population. Participants were recruited using random digit dialing between 1993 and 2001 with the following eligibility criteria: (1) age 40 or older, (2) clinically stroke free, and (3) resident of Northern Manhattan for at least 3 months. In person cognitive testing has been done three times since 2011 in surviving participants, Dementia was adjudicated by consensus between a neurologist and a neuropsychologist. The institutional review boards at Columbia University Medical Center and the University of Miami approved the study. All participants provided written informed consent.

Washington Heights–Inwood Columbia Aging Project (WHICAP study)

WHICAP is a prospective, population-based study of aging and dementia. Established through several recruitment waves, participants were first recruited in 1992 from a random sample of Medicare-eligible adults (age ≥65) residing in the neighborhoods of Washington Heights and Inwood in northern Manhattan. Participants are evaluated longitudinally every 18–24 months, with a comprehensive neuropsychological battery, medical and neurologic examination, and survey about health-related outcomes. [17] Dementia and dementia subtypes are adjudicated in a consensus conference that includes neurologists and neuropsychologists.

Epidemiology of Dementia In Singapore (EDIS study)

The EDIS study is a population-based cohort study conducted in southwestern Singapore between 2004 and 2011. It recruited participants who participated in the baseline visit of the Singapore Epidemiology of Eye Diseases (SEED) which comprised 10,033 adults of Chinese, Malay, and Indian ancestry, 40-80 years old [18-21]. Briefly, the EDIS study consisted of three independent population cohorts with a common protocol. In all studies, individuals 40-80 years old were selected by an age-stratified random sampling method from a computer-generated random list of names provided by the Ministry of Home Affairs. The study was approved by the SERI Institutional Review Board. Written informed consent was obtained, in the preferred language of participants, by bilingual study coordinators prior to recruitment into the study.

Memory Clinic in Singapore (MCS study)

The MCS study included patients attending the National University Hospital (NUH) and St Luke's Hospital memory clinics between 2009 and 2015. Patients were referred by primary care as well as secondary and tertiary care facilities because of consistent memory complaints and were assessed by a team of clinicians, psychologists, and nurses in the Memory Aging and Cognition Center, National University of Singapore.

Framingham Heart Study (FHS)

FHS started enrolling community-based participants in 1949. In 1971, all descendants of the original cohort (i.e., offspring cohort, requiring at least one parent from the original cohort) and their spouses were invited to participate in a follow-up study, and since then, they have been followed prospectively. The initial cohort consisted of 5124 men and women; 88% of survivors (3539/4031) participated in examination 7 in 1998-2001. Participants who survived to the 7th examination were invited to undergo a brain MRI (1999-2005), with a final sample of 2144 stroke-free, community-based participants. For these analyses, we used a FHS subsample with available MRA as part of the stroke case study.

Measurement of brain arterial diameter

Brain magnetic resonance angiogram acquisition parameters by cohort are reported in supplemental Table 1. Brain arterial diameters and lengths were obtained from all available MRA images using commercial software (LAVA, Leiden University Medical Center, The Netherlands, build date Oct 19, 2018). Briefly, this software uses a flexible 3D tubular Non-Uniform Rational B-Splines model to automatically identify the margins of the arterial lumen based on voxel intensity [22] with excellent reliability.[23] The 13 arterial segments measured included the bilateral intracranial internal carotid (ICA); middle cerebral (MCA), anterior cerebral (ACA), posterior cerebral (PCA), vertebral (VA), and posterior communicating (Pcomm) arteries, plus the basilar artery (BA). The location of measurement was aimed at the largest portion of a given segment free of focal stenosis, with good to excellent reliability. [24] For arteries visualized in the axial source MRA images but not large enough to be reconstructed, we systematically assigned the smallest measured diameters for the artery in the sample minus 10%. We counted arteries not visualized in axial source MRA images to create a score of absent arteries. We transformed each artery diameter distribution into normal scores and obtained the global (all 13 arteries), anterior (ICA, MCA, ACA and Pcomm if available) and posterior (VA, BA and PCA if available) arterial diameter scores by cohort as the principal dependent variable.

Genotyping and Imputation

Detailed description of genotyping, quality control and imputation in each study is provided in supplemental Table 2. All analyses were conducted on autosomal chromosomes. Genotypes with missing rate greater than 10%, significant Hardy-Weinberg Equilibrium p-value (HWE p-value $<5x10^{-8}$), or poor imputation quality ($r^2<0.3$) were excluded from the analyses.

Genome-wide Association Analysis

In each study and self-reported racial/ancestry strata, linear regression models were used to test the association between genetic variants and brain arterial diameter (global, anterior and posterior scores) using an additive genetic model, adjusted for sex, age, head size, number of absent arteries and population-specific principal components of ancestry (PCs). Genome-wide association studies (GWAS) results were subjected to quality control analyses using EasyQC (Winkler et al., 2013) and combined by meta-analysis using a fixed-effect inverse-variance-based method implemented in METAL [25] Variants with minor allele frequencies (MAF) < 1% and those do not present in at least two studies were excluded after the meta-analyses. Cross-study heterogeneity was assessed using Cochran's Q-test, and variants with heterogeneity p-value <0.05 were excluded. A trans-ancestry meta-analysis of GWAS was conducted to account for heterogeneity in allelic effect that is correlated with ancestry by Meta-Regression of Multi-Ethnic Genetic Association (MR-MEGA). [26] Ancestry-specific meta-analyses were also performed to identify ancestry-specific variants. Multi-Trait Analysis of GWAS (MTAG) tool [27] was used for multivariate analysis of anterior and posterior brain arterial diameter to boost the statistical power to detect genetic associations. An association with a p-value $< 5x10^{-8}$ was considered genome-wide significant, whereas p-value $< 1.0x10^{-5}$ were used as suggestive evidence for marker associations.

Gene-based Association Analysis and Gene-set Enrichment

We performed a gene-based association analysis based on summary statistics using Multi-marker Analysis of GenoMic Annotation (MAGMA v.1.07) ,[28] implemented by FUnctional Mapping and Annotation (FUMA).[29] Variants with p-value $< 1x10^{-5}$ were mapped to the nearest gene within 50kb or an expression quantitative trait locus (eQTL) genes in Genotype-Tissue Expression (GTEx) project data version 8 (v8)[30] from brain tissues: amygdala, anterior cingulate cortex (BA24), caudate (basal ganglia), cerebellar hemisphere, cerebellum, cortex, frontal Cortex (BA9), hippocampus, hypothalamus, nucleus accumbens (basal ganglia), putamen (basal ganglia), spinal cord (cervical c-1), substantia nigra. Mapped genes were then tested for tissue specificity in 30 general GTEx tissues using the pre-calculated differentially expressed gene (DEG) sets integrated in the GENE2FUNC of FUMA. [29] Hypergeometric enrichment tests were performed via GENE2FUNC against pre-defined gene sets obtained from Molecular signatures database (MsigDB) [31], WikiPathways [32] and GWAS catalog.[33] We used Bonferroni corrected p-value < 0.05 to define statistical significance in gene-based analyses.

Identification of Genomic Risk Loci and Deleteriousness of Lead SNPs

Variants that had at least suggestive evidence (p-value $<10^{-5}$) were filtered and LD-clumped at $r^2<0.1$ to identify independent loci using FUMA's SNP2GENE function [29] based on the relevant 1000G reference. To investigate the protein coding consequences of lead independent variants associated with brain arterial diameter, the Combined Annotation Dependent Depletion (CADD) score was estimated. We used the threshold of 12.37 to determine whether a lead variant was

deleterious. [34] When the CADD score of a lead variant was smaller than 12.37, we assessed whether its proxy variants (r^2>0.8) were deleterious instead.

Pleiotropic Association Analysis with Gene Expression

We used the SMR software [35] to test for pleiotropic association between brain arterial diameter traits and gene expression. We used summary-level data from our GWAS analyses and data on expression quantitative trait loci (eQTL) from the BrainMeta project version 2. [36] There are 5967 cis-eQTLs with eQTL p-value<5×10^{-8}. We used a Bonferroni corrected p-value < $8.4\text{x}10^{-6}$ (0.05/5967) to define statistical significance in pleiotropic association analyses.

Two Sample Mendelian Randomization Analysis

We conducted a two-sample Mendelian randomization (MR) analysis using genetic instruments from the present analyses to assess whether brain arterial diameter is a causal factor for Alzheimer's disease, stroke and white matter hyperintensities volume. The summary statistics for Alzheimer's disease, stroke and white matter hyperintensities volume were used in this analysis. [37-39] To avoid bias driven by correlated instruments, variants with brain arterial diameter association p-value <$1.0\text{x}10^{-5}$ were LD-clumped at r^2 < 0.01 [40] against the 1000 Genome LD reference calculated for African, European, Asian and Hispanic populations. Variants with MAFs < 0.01 in the reference population were excluded from MR analysis. Causal association was primarily evaluated using the inverse-variance weighted method. To assess the presence of horizontal pleiotropy (i.e, that variants influence the outcome trait via independent pathways other than the exposure trait), we used the simple mode method, weighted mode method, inverse-variance weighted method (IVW), median-based method, and MR-Egger method. All MR analyses were performed using the “TwoSampleMR” R package. [41]

Declarations

Ethics approval and consent to participate

The included studies have been approved by local ethics committees: Atherosclerosis Risk in Communities (ARIC) study: The institutional review board at The Johns Hopkins University, Wake Forest University, University of Mississippi Medical Center, and University of Minnesota; The Northern Manhattan Study (NOMAS): The institutional review boards at Columbia University Medical Center and the University of Miami; Washington Heights-Inwood Columbia Aging Project (WHICAP): The institutional review boards at Columbia University Medical Center; Epidemiology of Dementia In Singapore (EDIS): The institutional review boards at Singapore Eye Research Institute; Memory Clinic in Singapore (MCS): The institutional review boards at National University Hospital; Framingham Heart Study (FHS): The institutional review boards at Boston Medical Center.

Consent for publication

Informed consent has been obtained from all participants included in the analyzed studies.

Availability of data and materials

Studies participating in this meta-analysis have separate and specific data request and approval policies, depending on local, national, and international laws and regulations. Because of restrictions based on such privacy laws and regulations and informed consent of the participants, data cannot be made freely available in a public repository for any of the participating studies. Requests for information on procedures and formal data requests can be submitted to investigators from the corresponding author (Jose Gutierrez).

Competing interests

The authors declare that they have no competing interests.

Funding

This investigation was supported by National Institutes of Health grant R01 AG057709. The Atherosclerosis Risk in Communities (ARIC) Study is carried out as a collaborative study supported by National Heart, Lung, and Blood Institute contracts (75N92022D00001, 75N92022D00002, 75N92022D00003, 75N92022D00004, 75N92022D00005). The ARIC Neurocognitive Study is supported by U01HL096812, U01HL096814, U01HL096899, U01HL096902, and U01HL096917 from the NIH (NHLBI, NINDS, NIA and NIDCD). Funding was also supported by R01AG054491, R01HL087641 and R01HL086694; National Human Genome Research Institute contract U01HG004402; and National Institutes of Health contract HHSN268200625226C. Infrastructure was partly supported by Grant Number UL1RR025005, a component of the National Institutes of Health and NIH Roadmap for Medical Research. The Northern Manhattan Study (NOMAS) was supported by National Institutes of Health (R01 AG066162, R01 NS36286, R01 NS29993). The Washington Heights–Inwood Columbia Aging Project (WHICAP) was supported by National Institutes of Health (R01 AG072474, R01 AG037212, RF1 AG054023). The Epidemiology of Dementia In Singapore (EIDS) study was supported by the National Medical Research Council, Singapore (NMRC/CG/NUHS/2010 [Grant no: R-184-006-184-511]). The Memory Clinic in Singapore (MCS) was supported by U01 AG052409. The Framingham Heart Study (FHS) was supported by National Heart, Lung and Blood Institute contracts (N01 HC25195,

HHSN268201500001I, 75N92019D00031) with additional support from National Institutes of Health grants (R01 AG047645, R01 HL131029) and an American Heart Association Award (15GPSGC24800006).

Authors' contributions

ML performed statistical analyses, and drafted and revised the manuscript. FK, SS, AS, YQ, ET, SS, JR participated in data acquisition and revised the manuscript. DS, HA, QY, AB, SH, TR, JJ, GT participated in data analysis and interpretation and revised the manuscript. AB, ME, RS, CC, BW, MF were responsible for obtaining funding and revising the manuscript. JG was responsible for the study concept and design, obtaining funding, and drafting and revising the manuscript. All authors read and approved the final manuscript.

Acknowledgements

The authors thank the staff and participants of the ARIC, NOMAS, WHICAP, EDIS, MCS and FHS studies for their important contributions.

References

1. Morgagni G. *De sedibus et causis morborum per anatomen indigatis libri quinque. Venice: ex typographica Remondiana.* 1761.
2. Gutierrez J, Sacco RL, Wright CB. Dolichoectasia-an evolving arterial disease. *Nat Rev Neurol.* 2011;7(1):41-50.
3. Smoker WR, Corbett JJ, Gentry LR, Keyes WD, Price MJ, McKusker S. High-resolution computed tomography of the basilar artery: 2. Vertebrobasilar dolichoectasia: clinical-pathologic correlation and review. *AJNR Am J Neuroradiol.* 1986;7(1):61-72.
4. Gutierrez J, Bagci A, Gardener H, et al. Dolichoectasia diagnostic methods in a multi-ethnic, stroke-free cohort: results from the northern Manhattan study. *J Neuroimaging.* 2014;24(3):226-231.
5. Gutierrez J, Cheung K, Bagci A, et al. Brain Arterial Diameters as a Risk Factor for Vascular Events. *Journal of the American Heart Association.* 2015;4(8):e002289.
6. Gutierrez J, Guzman V, Khasiyev F, et al. Brain arterial dilatation and the risk of Alzheimer's disease. *Alzheimers Dement.* 2019;15(5):666-674.
7. Gutierrez J, Kulick E, Park Moon Y, et al. Brain Arterial Diameters and Cognitive Performance: The Northern Manhattan Study. *J Int Neuropsychol Soc.* 2017:1-12.
8. Pasterkamp G, Schoneveld AH, van Wolferen W, et al. The impact of atherosclerotic arterial remodeling on percentage of luminal stenosis varies widely within the arterial system. A postmortem study. *Arterioscler Thromb Vasc Biol.* 1997;17(11):3057-3063.
9. Xu WH, Li ML, Gao S, et al. In vivo high-resolution MR imaging of symptomatic and asymptomatic middle cerebral artery atherosclerotic stenosis. *Atherosclerosis.* 2010;212(2):507-511.
10. Groenink M, den Hartog AW, Franken R, et al. Losartan reduces aortic dilatation rate in adults with Marfan syndrome: a randomized controlled trial. *Eur Heart J.* 2013;34(45):3491-3500.
11. Morris SA, Orbach DB, Geva T, Singh MN, Gauvreau K, Lacro RV. Increased vertebral artery tortuosity index is associated with adverse outcomes in children and young adults with connective tissue disorders. *Circulation.* 2011;124(4):388-396.
12. Naunheim MR, Walcott BP, Nahed BV, MacRae CA, Levinson JR, Ogilvy CS. Arterial tortuosity syndrome with multiple intracranial aneurysms: a case report. *Arch Neurol.* 2011;68(3):369-371.

13. Gutierrez J, Bagci A, Del Brutto V, et al. Correlates of Dolichoectasia in an Urban, Stroke-free Cohort: Results From the Northern Manhattan Study. *Stroke.* 2014;45(Suppl 1):ATP152.
14. Gutierrez J, DiTullio M, K Cheung YK, et al. Brain arterial dilatation modifies the association between extracranial pulsatile hemodynamics and brain perivascular spaces: the Northern Manhattan Study. *Hypertension Research.* 2019.
15. Wright JD, Folsom AR, Coresh J, et al. The ARIC (Atherosclerosis Risk In Communities) Study. *Journal of the American College of Cardiology.* 2021;77(23):2939-2959.
16. Knopman DS, Gottesman RF, Sharrett AR, et al. Mild Cognitive Impairment and Dementia Prevalence: The Atherosclerosis Risk in Communities Neurocognitive Study (ARIC-NCS). *Alzheimer's & dementia (Amsterdam, Netherlands).* 2016;2:1-11.
17. Manly JJ, Bell-McGinty S, Tang MX, Schupf N, Stern Y, Mayeux R. Implementing diagnostic criteria and estimating frequency of mild cognitive impairment in an urban community. *Archives of neurology.* 2005;62(11):1739-1746.
18. Foong AW, Saw SM, Loo JL, et al. Rationale and methodology for a population-based study of eye diseases in Malay people: The Singapore Malay eye study (SiMES). *Ophthalmic epidemiology.* 2007;14(1):25-35.
19. Lavanya R, Jeganathan VS, Zheng Y, et al. Methodology of the Singapore Indian Chinese Cohort (SICC) eye study: quantifying ethnic variations in the epidemiology of eye diseases in Asians. *Ophthalmic epidemiology.* 2009;16(6):325-336.
20. Wong TY, Chong EW, Wong WL, et al. Prevalence and causes of low vision and blindness in an urban malay population: the Singapore Malay Eye Study. *Archives of ophthalmology (Chicago, Ill : 1960).* 2008;126(8):1091-1099.
21. Zheng Y, Lavanya R, Wu R, et al. Prevalence and causes of visual impairment and blindness in an urban Indian population: the Singapore Indian Eye Study. *Ophthalmology.* 2011;118(9):1798-1804.
22. Suinesiaputra A, de Koning PJ, Zudilova-Seinstra E, Reiber JH, van der Geest RJ. Automated quantification of carotid artery stenosis on contrast-enhanced MRA data using a deformable vascular tube model. *Int J Cardiovasc Imaging.* 2012;28(6):1513-1524.
23. Qiao Y, Guallar E, Suri FK, et al. MR Imaging Measures of Intracranial Atherosclerosis in a Population-based Study. *Radiology.* 2016;280(3):860-868.
24. Gutierrez J, Khasiyev F, Liu M, et al. Determinants and Outcomes of Asymptomatic Intracranial Atherosclerotic Stenosis. *J Am Coll Cardiol.* 2021;78(6):562-571.
25. Willer CJ, Li Y, Abecasis GR. METAL: fast and efficient meta-analysis of genomewide association scans. *Bioinformatics.* 2010;26(17):2190-2191.
26. Magi R, Horikoshi M, Sofer T, et al. Trans-ethnic meta-regression of genome-wide association studies accounting for ancestry increases power for discovery and improves fine-mapping resolution. *Human molecular genetics.* 2017;26(18):3639-3650.
27. Turley P, Walters RK, Maghzian O, et al. Multi-trait analysis of genome-wide association summary statistics using MTAG. *Nature genetics.* 2018;50(2):229-237.
28. de Leeuw CA, Mooij JM, Heskes T, Posthuma D. MAGMA: generalized gene-set analysis of GWAS data. *PLoS Comput Biol.* 2015;11(4):e1004219.
29. Watanabe K, Taskesen E, van Bochoven A, Posthuma D. Functional mapping and annotation of genetic associations with FUMA. *Nat Commun.* 2017;8(1):1826.
30. Consortium GT. Human genomics. The Genotype-Tissue Expression (GTEx) pilot analysis: multitissue gene regulation in humans. *Science.* 2015;348(6235):648-660.
31. Liberzon A, Birger C, Thorvaldsdottir H, Ghandi M, Mesirov JP, Tamayo P. The Molecular Signatures Database (MSigDB) hallmark gene set collection. *Cell Syst.* 2015;1(6):417-425.
32. Slenter DN, Kutmon M, Hanspers K, et al. WikiPathways: a multifaceted pathway database bridging metabolomics to other omics research. *Nucleic Acids Res.* 2018;46(D1):D661-D667.

33. Buniello A, MacArthur JAL, Cerezo M, et al. The NHGRI-EBI GWAS Catalog of published genome-wide association studies, targeted arrays and summary statistics 2019. *Nucleic Acids Res.* 2019;47(D1):D1005-D1012.
34. Kircher M, Witten DM, Jain P, O'Roak BJ, Cooper GM, Shendure J. A general framework for estimating the relative pathogenicity of human genetic variants. *Nature genetics.* 2014;46(3):310-315.
35. Zhu Z, Zhang F, Hu H, et al. Integration of summary data from GWAS and eQTL studies predicts complex trait gene targets. *Nature genetics.* 2016;48(5):481-487.
36. Qi T, Wu Y, Zeng J, et al. Identifying gene targets for brain-related traits using transcriptomic and methylomic data from blood. *Nat Commun.* 2018;9(1):2282.
37. Bellenguez C, Küçükali F, Jansen IE, et al. New insights into the genetic etiology of Alzheimer's disease and related dementias. *Nature genetics.* 2022;54(4):412-436.
38. Malik R, Rannikmäe K, Traylor M, et al. Genome-wide meta-analysis identifies 3 novel loci associated with stroke. *Ann Neurol.* 2018;84(6):934-939.
39. Elliott LT, Sharp K, Alfaro-Almagro F, et al. Genome-wide association studies of brain imaging phenotypes in UK Biobank. *Nature.* 2018;562(7726):210-216.
40. Davies NM, Hill WD, Anderson EL, Sanderson E, Deary IJ, Davey Smith G. Multivariable two-sample Mendelian randomization estimates of the effects of intelligence and education on health. *eLife.* 2019;8.
41. Hemani G, Zheng J, Elsworth B, et al. The MR-Base platform supports systematic causal inference across the human phenome. *eLife.* 2018;7.
42. Volpe SL. Magnesium in disease prevention and overall health. *Advances in nutrition (Bethesda, Md).* 2013;4(3):378s-383s.
43. Accogli A, Scala M, Calcagno A, et al. CNNM2 homozygous mutations cause severe refractory hypomagnesemia, epileptic encephalopathy and brain malformations. *Eur J Med Genet.* 2019;62(3):198-203.
44. Stuiver M, Lainez S, Will C, et al. CNNM2, encoding a basolateral protein required for renal Mg2+ handling, is mutated in dominant hypomagnesemia. *American journal of human genetics.* 2011;88(3):333-343.
45. Steen H, Lindholm D. Nuclear localized protein-1 (Nulp1) increases cell death of human osteosarcoma cells and binds the X-linked inhibitor of apoptosis protein. *Biochemical and biophysical research communications.* 2008;366(2):432-437.
46. Duarte RRR, Bachtel ND, Cotel MC, et al. The Psychiatric Risk Gene NT5C2 Regulates Adenosine Monophosphate-Activated Protein Kinase Signaling and Protein Translation in Human Neural Progenitor Cells. *Biol Psychiatry.* 2019;86(2):120-130.
47. Singgih EL, van der Voet M, Schimmel-Naber M, Brinkmann EL, Schenck A, Franke B. Investigating cytosolic 5'-nucleotidase II family genes as candidates for neuropsychiatric disorders in Drosophila (114/150 chr). *Translational psychiatry.* 2021;11(1):55.
48. Itoh R. Enzymatic properties and physiological roles of cytosolic 5'-nucleotidase II. *Curr Med Chem.* 2013;20(34):4260-4284.
49. Hoffman GE, Schrode N, Flaherty E, Brennand KJ. New considerations for hiPSC-based models of neuropsychiatric disorders. *Mol Psychiatry.* 2019;24(1):49-66.
50. Tang Y, Illes P. Regulation of adult neural progenitor cell functions by purinergic signaling. *Glia.* 2017;65(2):213-230.
51. Tornroth-Horsefield S, Neutze R. Opening and closing the metabolite gate. *Proceedings of the National Academy of Sciences of the United States of America.* 2008;105(50):19565-19566.
52. Kulkarni SS, Karlsson HK, Szekeres F, Chibalin AV, Krook A, Zierath JR. Suppression of 5'-nucleotidase enzymes promotes AMP-activated protein kinase (AMPK) phosphorylation and metabolism in human and mouse skeletal muscle. *J Biol Chem.* 2011;286(40):34567-34574.
53. Chen X, Zhang Z, Wang X, Chen Y, Wang C. NT5C2 Gene Polymorphisms and the Risk of Coronary Heart Disease. *Public health genomics.* 2020;23(3-4):90-99.

54. Li Z, Jiang J, Long J, et al. The rs11191580 variant of the NT5C2 gene is associated with schizophrenia and symptom severity in a South Chinese Han population: evidence from GWAS. *Revista brasileira de psiquiatria (Sao Paulo, Brazil : 1999).* 2017;39(2):104-109.
55. Vishnolia KK, Hoene C, Tarhbalouti K, Revenstorff J, Aherrahrou Z, Erdmann J. Studies in Zebrafish Demonstrate That CNNM2 and NT5C2 Are Most Likely the Causal Genes at the Blood Pressure-Associated Locus on Human Chromosome 10q24.32. *Front Cardiovasc Med.* 2020;7:135.
56. Lin S, Shi Q, Nix FB, et al. A novel S-adenosyl-L-methionine:arsenic(III) methyltransferase from rat liver cytosol. *J Biol Chem.* 2002;277(13):10795-10803.
57. Liu WS, Wang XY, Lu J, et al. Polymorphisms in arsenic (+□3 oxidation state) methyltransferase (AS3MT) predict the occurrence of hyperleukocytosis and arsenic metabolism in APL patients treated with As(2)O(3). *Archives of toxicology.* 2020;94(4):1203-1213.
58. Su AI, Cooke MP, Ching KA, et al. Large-scale analysis of the human and mouse transcriptomes. *Proceedings of the National Academy of Sciences of the United States of America.* 2002;99(7):4465-4470.
59. Li M, Jaffe AE, Straub RE, et al. A human-specific AS3MT isoform and BORCS7 are molecular risk factors in the 10q24.32 schizophrenia-associated locus. *Nat Med.* 2016;22(6):649-656.
60. Zhao W, Zhang Q, Chen X, et al. The VNTR of the AS3MT gene is associated with brain activations during a memory span task and their training-induced plasticity. *Psychological medicine.* 2021;51(11):1927-1932.
61. Duarte RRR, Troakes C, Nolan M, Srivastava DP, Murray RM, Bray NJ. Genome-wide significant schizophrenia risk variation on chromosome 10q24 is associated with altered cis-regulation of BORCS7, AS3MT, and NT5C2 in the human brain. *American journal of medical genetics Part B, Neuropsychiatric genetics: the official publication of the International Society of Psychiatric Genetics.* 2016;171(6):806-814.
62. Guan F, Zhang T, Li L, et al. Two-stage replication of previous genome-wide association studies of AS3MT-CNNM2-NT5C2 gene cluster region in a large schizophrenia case-control sample from Han Chinese population. *Schizophrenia research.* 2016;176(2-3):125-130.
63. Navone F, Genevini P, Borgese N. Autophagy and Neurodegeneration: Insights from a Cultured Cell Model of ALS. *Cells.* 2015;4(3):354-386.
64. Menzies FM, Fleming A, Caricasole A, et al. Autophagy and Neurodegeneration: Pathogenic Mechanisms and Therapeutic Opportunities. *Neuron.* 2017;93(5):1015-1034.
65. Pu J, Schindler C, Jia R, Jarnik M, Backlund P, Bonifacino JS. BORC, a multisubunit complex that regulates lysosome positioning. *Developmental cell.* 2015;33(2):176-188.
66. Jia R, Guardia CM, Pu J, Chen Y, Bonifacino JS. BORC coordinates encounter and fusion of lysosomes with autophagosomes. *Autophagy.* 2017;13(10):1648-1663.
67. Snouwaert JN, Church RJ, Jania L, et al. A Mutation in the Borcs7 Subunit of the Lysosome Regulatory BORC Complex Results in Motor Deficits and Dystrophic Axonopathy in Mice. *Cell reports.* 2018;24(5):1254-1265.
68. Mitra AK, Crews KR, Pounds S, et al. Genetic variants in cytosolic 5'-nucleotidase II are associated with its expression and cytarabine sensitivity in HapMap cell lines and in patients with acute myeloid leukemia. *J Pharmacol Exp Ther*. 2011;339(1), 9-23.

Tables

Table 1 Demographic information of studies

Cohort	ARIC	NOMAS	WHICAP	EDIS	MCS	FHS
N	1565	1092	290	647	350	206
Age, years, mean (sd)	75.8 (5.3)	70.1 (8.4)	77.2 (6.5)	70.2 (6.6)	71.0 (8.2)	72.7 (11.7)
Female (%)	58.8	60.5	64.1	51.7	55.7	54.3
Self-reported racial/ethnic identity or geographic ancestry (%)						
European/white	74.3	13.8	44.8	-	-	100.0
African/black/African American	25.7	16.6	55.2	-	-	-
Hispanic	-	69.6	-	-	-	-
Asian	-	-	-	100.0	100.0	-
Hypertension (%)	74.9	68.1	63.1	80.8	67.8	68.4
Diabetes (%)	33.9	19.0	20.2	37.3	31.8	23.9
Dyslipidemia (%)	56.0	45.0	33.9	76.0	71.4	51.6
Smoking (%)	6.0	52.7	5.2	27.9	7.1	9.3

ARIC, Atherosclerosis Risk in Communities study; NOMAS, The Northern Manhattan Study; WHICAP, Washington Heights-Inwood Community Aging Project; EIDS, Epidemiology of Dementia In Singapore; MCS, Memory Clinic in Singapore; FHS, Framingham Heart Study.

Table 2 Variants ($P < 5\times10^{-8}$) associated with brain arterial diameter

SNP	Chr	Position (hg 19)	Nearest gene	Relation to gene	Allele1	Allele2	AF	beta	se	P value	CADD
Global											
rs7921574	10	104840970	CNNM2	ncRNA_intronic	C	T	0.42	0.06	0.01	1.54E-08	0.33
rs943035	10	104839152	CNNM2	ncRNA_intronic	C	T	0.42	0.06	0.01	1.57E-08	0.71
rs10883826*	10	104830819	CNNM2	ncRNA_intronic	G	A	0.42	0.06	0.01	1.58E-08	2.25
rs943036	10	104836047	CNNM2	ncRNA_intronic	C	T	0.42	0.06	0.01	1.66E-08	5.85
rs10883824	10	104812897	CNNM2	ncRNA_intronic	G	A	0.42	0.06	0.01	2.12E-08	2.98
rs8139	10	104848123	CNNM2	ncRNA_intronic	A	G	0.42	0.06	0.01	2.31E-08	7.82
rs3740387	10	104849468	CNNM2	ncRNA_intronic	A	G	0.42	0.06	0.01	2.33E-08	8.71
rs10883817	10	104755431	CNNM2	ncRNA_intronic	A	G	0.42	0.06	0.01	2.82E-08	0.37
rs3902934	10	104746649	CNNM2	ncRNA_intronic	G	A	0.42	0.06	0.01	2.84E-08	1.24
rs10883823	10	104812331	CNNM2	ncRNA_intronic	C	T	0.42	0.06	0.01	3.35E-08	0.25
rs7911789	10	104756374	CNNM2	ncRNA_intronic	C	T	0.42	0.06	0.01	3.84E-08	0.58
rs67908413	10	104764989	CNNM2	ncRNA_intronic	C	T	0.42	0.06	0.01	3.84E-08	6.84
rs1890184	10	104748459	CNNM2	ncRNA_intronic	C	A	0.42	0.06	0.01	4.26E-08	0.62
rs10786733	10	104794947	CNNM2	ncRNA_intronic	A	G	0.42	0.06	0.01	4.84E-08	4.21
Posterior											
rs35994878	16	89949033	TCF25	Intronic	C	T	0.29	0.11	0.02	2.94E-08	1.06
rs8061025	16	89948397	TCF25	Intronic	A	G	0.29	0.11	0.02	4.49E-08	0.42

* Independent variant associated with brain arterial diameter. Nearest gene with a functional protein or RNA product that either overlaps with the variant or for intergenic variants, the nearest genes up- and downstream, respectively. The statistics are based on Allele1. Allele1 indicates effect allele, allele2 is another allele. AF: allele 1 frequency. CADD, combined annotation dependent depletion score. Chr, chromosome.

Table 3 Trans-ancestry Genome-Wide Significant Associations

SNP	Chr	Position (hg 19)	Nearest gene	Relation to gene	Allele1	Allele2	AF	P value	P_Het ANCS	P_Res Het	CADD
Global											
rs10883805	10	104708251	CNNM2	ncRNA_intronic	C	T	0.43	1.88E-08	0.003	0.333	4.39
rs10748839	10	104953547	NT5C2	upstream	C	T	0.42	2.54E-08	0.001	0.526	3.34
rs3902934	10	104746649	CNNM2	ncRNA_intronic	G	A	0.42	4.55E-08	0.026	0.329	1.24
rs10883814	10	104737404	CNNM2	ncRNA_intronic	C	T	0.43	4.79E-08	0.004	0.324	3.01
rs12569617	10	104729996	CNNM2	ncRNA_intronic	C	T	0.43	4.85E-08	0.004	0.323	2.87
rs10786721	10	104654383	AS3MT	ncRNA_intronic	A	C	0.43	4.97E-08	0.004	0.384	4.52
Anterior											
rs34217249	7	960642	ADAP1	Intronic	A	G	0.20	3.11E-08	2.03E-08	0.36	2.26

Nearest gene with a functional protein or RNA product that either overlaps with the variant or for intergenic variants, the nearest genes up- and downstream, respectively. The statistics are based on Allele1. Allele1 indicates effect allele, allele2 is another allele. AF: allele 1 frequency. CADD, combined annotation dependent depletion score. Chr, chromosome. P_Het ANCS P-value for heterogeneity correlated with ancestry. P_Res Het is the residual heterogeneity.

Table 4 Top 10 Co-localization of brain arterial diameter GWAS and eQTL associations

Probe ID	Probe Chr	Gene	Probe_bp	SNP	SNP chr	SNP bp	Allele1	Allele2	AF	beta	se	p
Global												
ENSG00000148842.18	10	CNNM2	104764015	rs7897654	10	104662458	C	T	0.28	0.12	0.02	6.17E-07*
ENSG00000272912.1	10	AL356608.1	104674752	rs10786719	10	104637992	G	A	0.41	-0.17	0.04	6.60E-06*
ENSG00000137760.15	11	ALKBH8	107404960	rs2037827	11	107408592	C	T	0.21	-0.11	0.03	3.22E-04
ENSG00000186715.11	1	MST1L	17089068	rs7513616	1	17298496	G	A	0.43	-0.06	0.02	6.88E-04
ENSG00000140265.12	15	ZSCAN29	43656796	rs523156	15	43811843	G	C	0.53	0.08	0.03	7.75E-04
ENSG00000014123.10	6	UFL1	96986312	rs11153023	6	96968525	T	C	0.15	-0.12	0.03	8.19E-04
ENSG00000237624.1	1	OXCT2P1	39981395	rs12028034	1	40039707	A	G	0.24	0.08	0.02	8.29E-04
ENSG00000159363.19	1	ATP13A2	17325438	rs7513616	1	17298496	G	A	0.43	0.09	0.03	8.53E-04
ENSG00000065717.15	19	TLE2	3022635	rs11150	19	2997897	A	G	0.17	-0.17	0.05	9.46E-04
ENSG00000268869.6	1	ESPNP	17030243	rs7513616	1	17298496	G	A	0.43	-0.12	0.04	1.36E-03
Anterior												
ENSG00000272912.1	10	AL356608.1	104674752	rs10786719	10	104637992	G	A	0.41	-0.17	0.04	4.98E-05
ENSG00000148842.18	10	CNNM2	104764015	rs7897654	10	104662458	C	T	0.28	0.10	0.02	6.62E-05
ENSG00000162669.16	1	HFM1	91798368	rs17131417	1	91848784	T	C	0.11	0.06	0.02	7.78E-05
ENSG00000162461.8	1	SLC25A34	16065320	rs41393951	1	16053493	A	G	0.31	-0.05	0.01	3.75E-04
ENSG00000137760.15	11	ALKBH8	107404960	rs2037827	11	107408592	C	T	0.21	-0.11	0.03	3.79E-04
ENSG00000065060.17	6	UHRF1BP1	34805354	rs6906129	6	34801160	C	T	0.51	-0.05	0.02	4.60E-04
ENSG00000156052.11	9	GNAQ	80488870	rs4582625	9	80520544	C	T	0.26	-0.08	0.02	6.44E-04
ENSG00000257354.2	12	AC048341.1	63006262	rs17731893	12	63013773	A	G	0.18	0.27	0.08	6.70E-04
ENSG00000231305.4	3	AC112484.1	128584923	rs789217	3	128593201	A	G	0.26	0.04	0.01	7.64E-04
ENSG00000016402.13	6	IL20RA	137343712	rs9494644	6	137403294	G	C	0.31	0.21	0.06	7.80E-04
Posterior												
ENSG00000138111.14	10	MFSD13A	104228977	rs11593583	10	104228149	G	A	0.56	-0.16	0.04	1.23E-04
ENSG00000168386.18	3	FILIP1L	99691171	rs6809988	3	99656615	A	G	0.22	0.13	0.03	2.75E-04
ENSG00000213903.9	14	LTB4R	24783949	rs11158632	14	24769663	G	T	0.22	-0.23	0.06	4.01E-04
ENSG00000148842.18	10	CNNM2	104764015	rs7897654	10	104662458	C	T	0.28	0.11	0.03	4.11E-04

ENSG00000223959.8	16	AFG3L1P	90053782	rs2270459	16	89979851	A	C	0.11	-0.21	0.06	4.48E-04
ENSG00000111615.14	12	KRR1	75895030	rs2070162	12	75900588	G	A	0.25	-0.06	0.02	4.60E-04
ENSG00000214043.8	12	LINC02347	126940360	rs17577161	12	126842742	G	A	0.34	0.06	0.02	5.97E-04
ENSG00000255595.5	12	AC007368.1	126797235	rs17577161	12	126842742	G	A	0.34	-0.07	0.02	6.18E-04
ENSG00000258839.4	16	MC1R	89982954	rs2270459	16	89979851	A	C	0.11	0.22	0.06	6.36E-04
ENSG00000256310.1	12	NDUFA5P6	127008983	rs17577161	12	126842742	G	A	0.34	0.09	0.02	6.78E-04

Allele1 indicates effect allele, allele2 is another allele. AF: allele 1 frequency. *Significant functional genes at P value < 8.4E-06

Figures

A

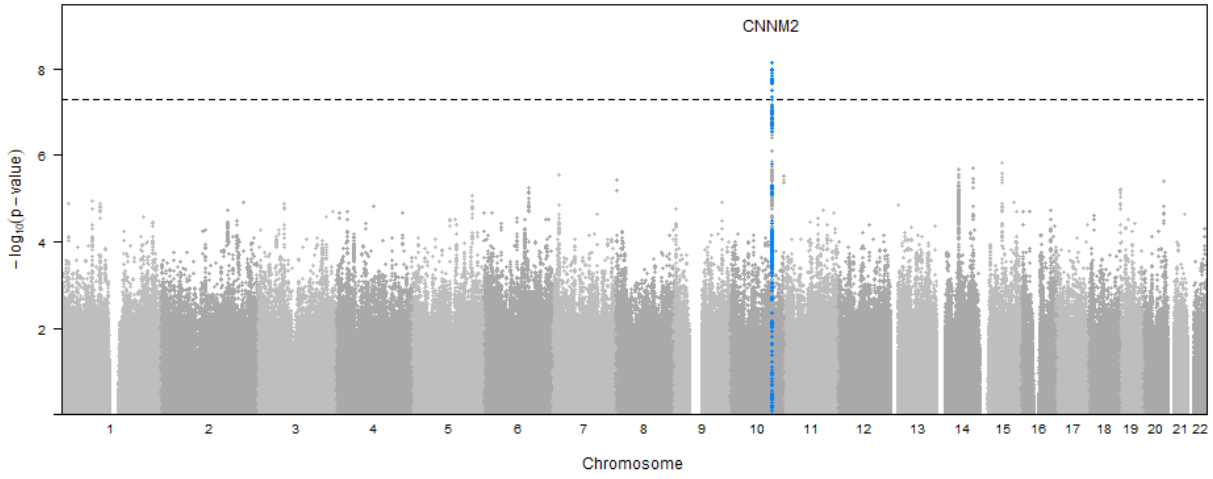
CNNM2
8
6
4
2
$-\log_{10}(p-value)$
1 2 3 4 5 6 7 8 9 10 11 12 13 14 15 16 17 18 19 20 21 22
Chromosome

B

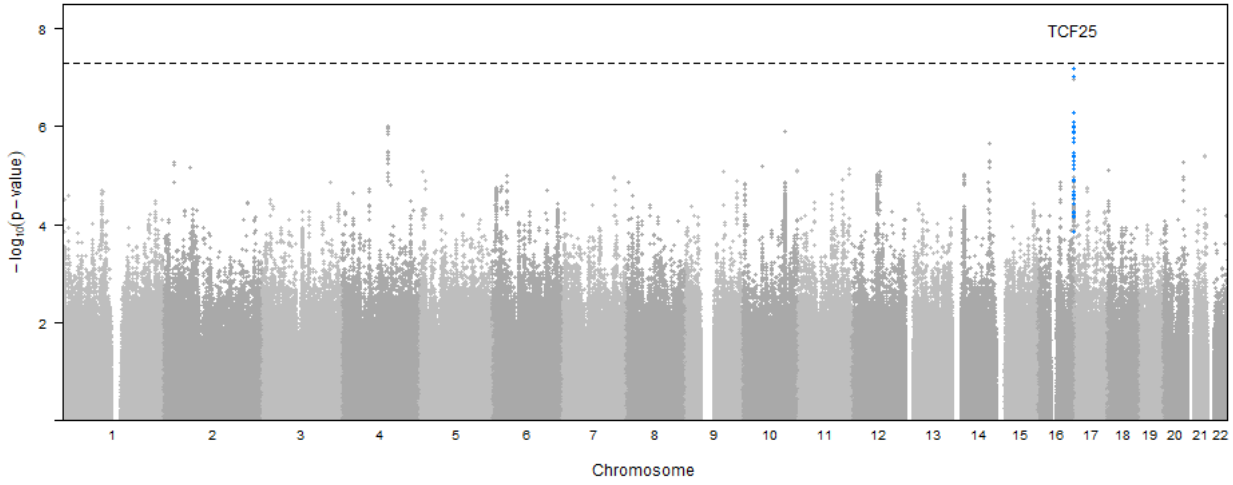
TCF25
8
6
4
2
$-\log_{10}(p-value)$
1 2 3 4 5 6 7 8 9 10 11 12 13 14 15 16 17 18 19 20 21 22
Chromosome

C

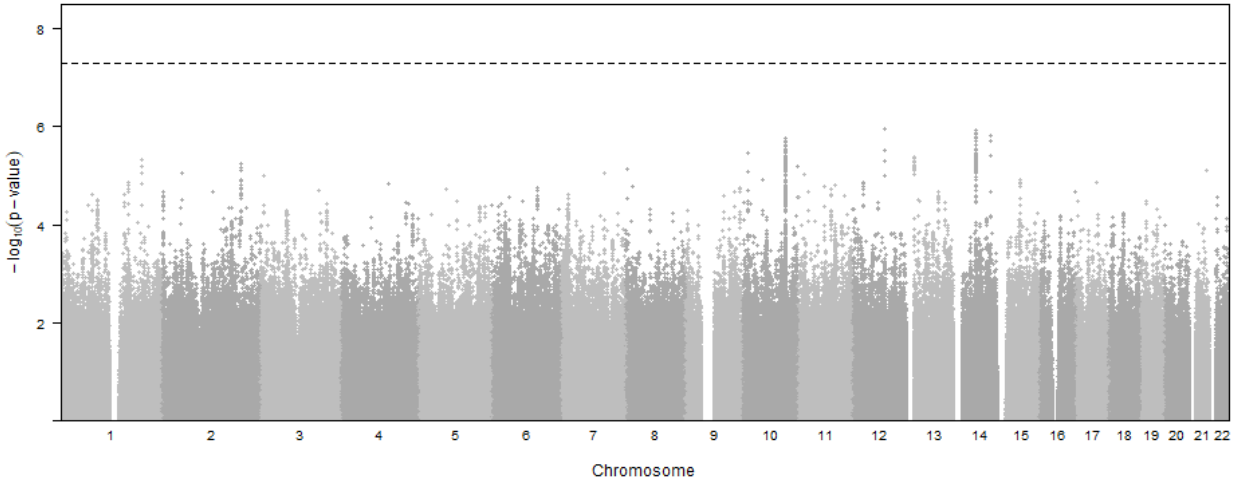

Figure 1 Genome-wide associations in brain arterial diameter.
Manhattan plots for brain arterial diameter show combined genome-wide associations from 6 population-based studies.

A

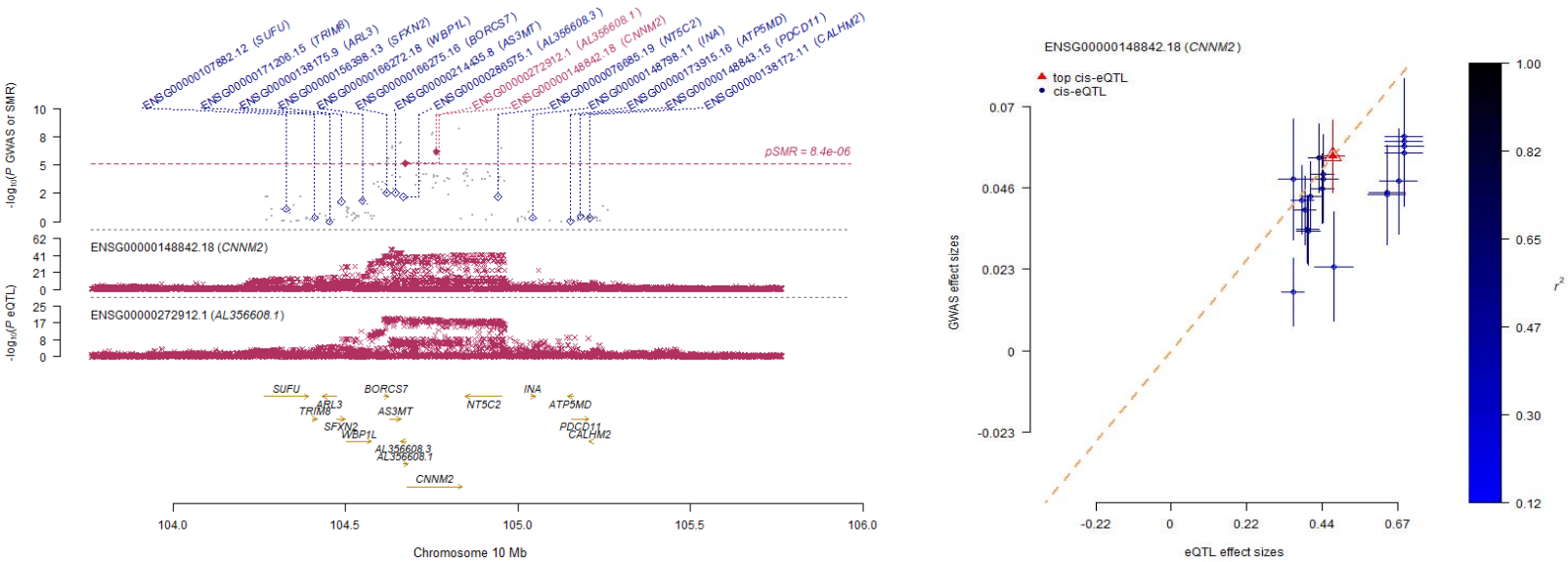
ENSG00000107882.12 (SUFU)
ENSG00000171206.15 (TRIM8)
ENSG00000138175.9 (ARL3)
ENSG00000156398.13 (SFXN2)
ENSG00000166272.18 (WBP1L)
ENSG00000166275.16 (BORCS7)
ENSG00000214435.8 (AS3MT)
ENSG00000286575.1 (AL356608.3)
ENSG00000272912.1 (AL356608.1)
ENSG00000148842.18 (CNNM2)
ENSG00000076685.19 (NT5C2)
ENSG00000148798.11 (INA)
ENSG00000173915.16 (ATP5MD)
ENSG00000148843.15 (PDCD11)
ENSG00000138172.11 (CALHM2)
-log10(P GWAS or SMR)
pSMR = 8.4e-06
ENSG00000148842.18 (CNNM2)
ENSG00000272912.1 (AL356608.1)
-log10(P eQTL)
SUFU
BORCS7
INA
ARL3
TRIM8
AS3MT
NT5C2
ATP5MD
SFXN2
WBP1L
PDCD11
CALHM2
AL356608.3
AL356608.1
CNNM2
Chromosome 10 Mb
ENSG00000148842.18 (CNNM2)
top cis-eQTL
cis-eQTL
GWAS effect sizes
eQTL effect sizes
r2

B

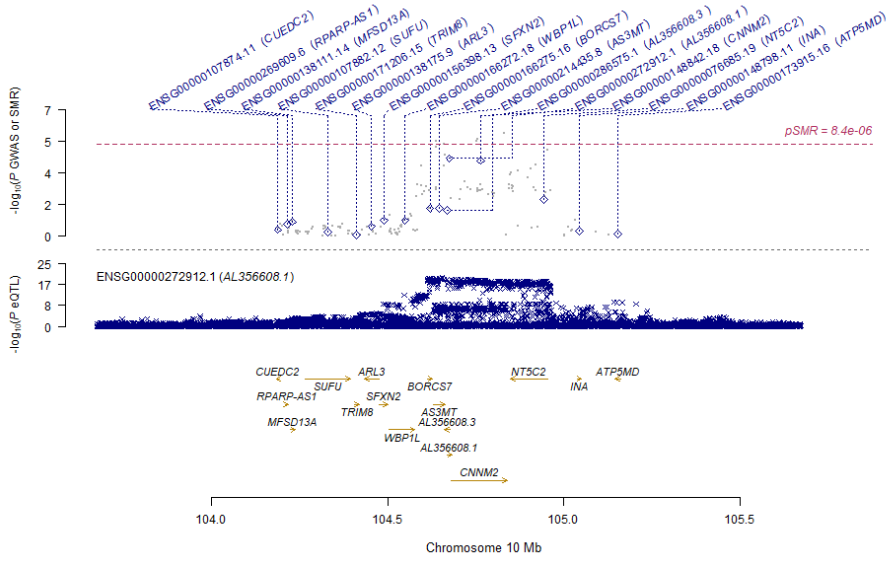
ENSG00000107874.11 (CUEDC2)
ENSG00000269609.6 (RPARP-AS1)
ENSG00000138111.14 (MFSD13A)
ENSG00000107882.12 (SUFU)
ENSG00000171206.15 (TRIM8)
ENSG00000138175.9 (ARL3)
ENSG00000156398.13 (SFXN2)
ENSG00000166272.18 (WBP1L)
ENSG00000166275.16 (BORCS7)
ENSG00000214435.8 (AS3MT)
ENSG00000286575.1 (AL356608.3)
ENSG00000272912.1 (AL356608.1)
ENSG00000148842.18 (CNNM2)
ENSG00000076685.19 (NT5C2)
ENSG00000148798.11 (INA)
ENSG00000173915.16 (ATP5MD)
pSMR = 8.4e-06
-log10(P GWAS or SMR)
-log10(P eQTL)
ENSG00000272912.1 (AL356608.1)
CUEDC2
SUFU
ARL3
BORCS7
NT5C2
ATP5MD
INA
RPARP-AS1
SFXN2
TRIM8
AS3MT
AL356608.3
MFSD13A
WBP1L
AL356608.1
CNNM2
104.0
104.5
105.0
105.5
Chromosome 10 Mb

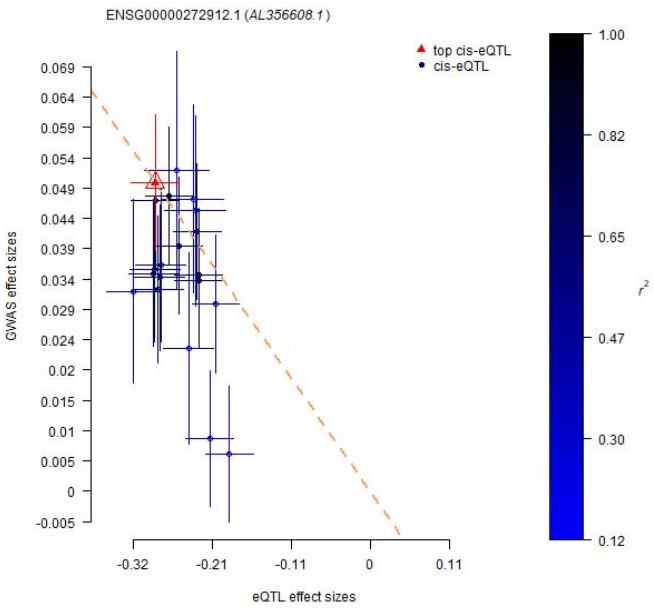
ENSG00000272912.1 (AL356608.1)
top cis-eQTL
cis-eQTL
GWAS effect sizes
eQTL effect sizes
-0.32
-0.21
-0.11
0
0.11
r2
1.00
0.82
0.65
0.47
0.30
0.12

C

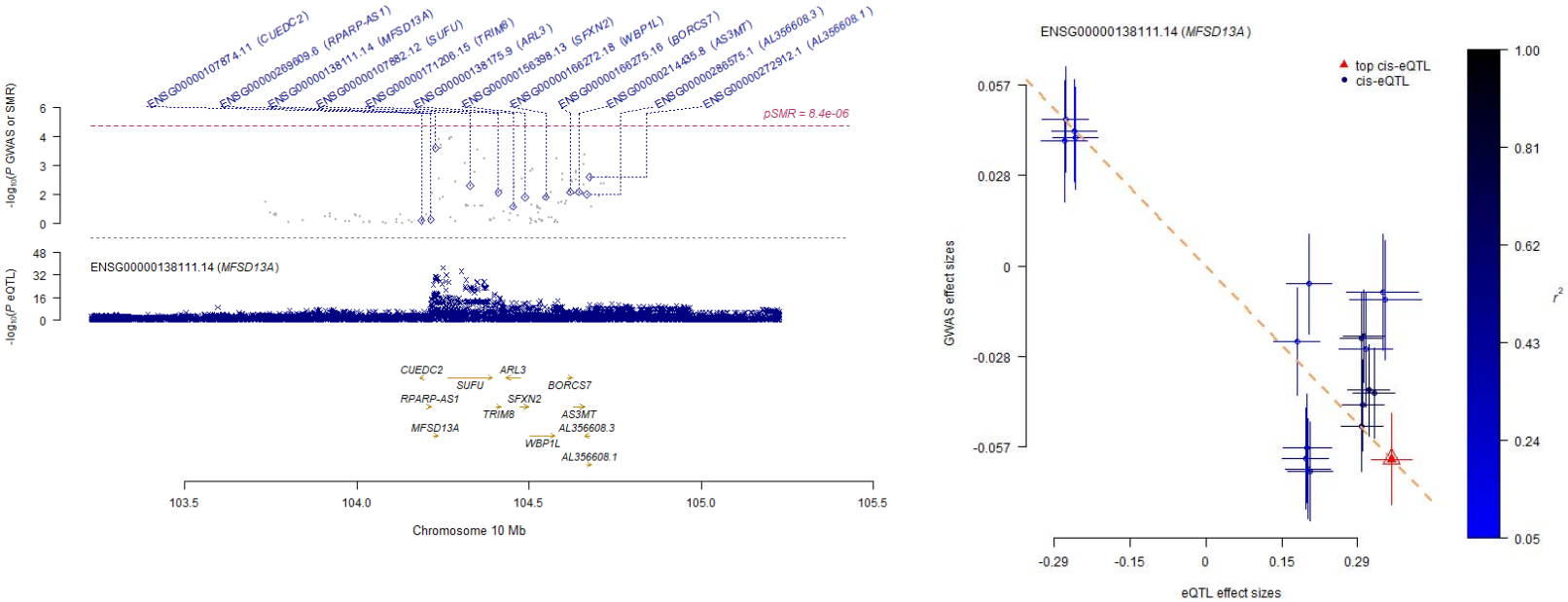

Figure 2 Locus plot and effect sizes plot of genome-wide association studies (GWAS) and expression quantitative trait locus (eQTL) associations.